Case Report

A paediatric dysembryoplastic neuroepithelial tumour (DNET) with deregulated stem cell markers: a case report

Deema Hussein[1#], Alazouf Alhowity[1#], Rinad Algehani[1], Abdulla Ahmed A. Salwati[1], Ashraf Dallol[2], Hans-Juergen Schulten[2], Saleh Baeesa[3], Mohammed Bangash[3], Fahad Alghamdi[4], Mohamad Saka[1], Adeel Chaudhary[5], Adel Abuzenadah[1,2,5]

[1]King Fahd Medical Research Center (KFMRC), Department of Medical Laboratory Technology, Faculty of Applied Medical Sciences, King Abdulaziz University, Jeddah, Saudi Arabia; [2]Center of Excellence in Genomic Medicine Research, Department of Medical Laboratory Technology, Faculty of Applied Medical Sciences, King Abdulaziz University, Jeddah, Saudi Arabia; [3]Division of Neurosurgery, Faculty of Medicine, King Abdulaziz University, Jeddah, Saudi Arabia; [4]Department of Pathology, Faculty of Medicine, King Abdulaziz University, Jeddah, Saudi Arabia; [5]Centre of Innovation for Personalised Medicine, Department of Medical Laboratory Technology, Faculty of Applied Medical Sciences, King Abdulaziz University, Jeddah, Saudi Arabia

[#]These authors contributed equally to this work and should be considered as co-first authors.

Correspondence to: Deema Hussein, BS, PhD. King Fahd Medical Research Center, King Abdulaziz University, Jeddah 21589, P.O. Box. 80216, Saudi Arabia. Email: deemah@hotmail.com; dmhussein@kau.edu.sa.

Background: Dysembryoplastic neuroepithelial tumours (DNETs) are rare, with only a few reported lethal cases. Currently, there are focused efforts by neuro-oncology professionals to reveal the molecular characterisations of individual central nervous system tumours (CNSTs). Here, we report the status of cancer stem cell (CSC) genes associated with resilience and drug resistance in a paediatric DNET, since the deregulations and variations of CSC genes may prove critical to these tumours' molecular characterisations.

Case Description: Immunofluorescence, clonogenic assay and whole exome sequencing (WES) were applied to the patient's tissue and its corresponding cell line. The case is for of a 6-year-old boy with intractable epilepsy and unremarkable physical and neurological examinations. Following magnetic resonance imaging (MRI) and histopathological tests, the patient was diagnosed with DNET. The child underwent a right posterior temporoparietooccipital neuronavigation-assisted craniotomy. Several CSC markers were upregulated *in situ*, including the metastasis-related protein, anterior gradient 2 (AGR2; 67%), and the Wnt-signalling-related protein, frizzled class receptor 9 (FZD9; 79%). The cell line possessed a similar DNA profile as the original tissue, stained positive for the tumorigenic marker [BMI1 proto-oncogene (BMI)] and CSC markers, and displayed drug resistance. Variants identified in the tissue DNA, which are listed in the catalogue of somatic mutations in cancer (COSMIC) database for genes previously known to be necessary for the development of the embryonic brain, included variants in the cell division cycle 27 (*CDC27*) gene.

Conclusions: we report the *in situ* and *in vitro* presence of CSCs in a paediatric DNET.

Keywords: Case report; central nervous system tumour (CNST); dysembryoplastic neuroepithelial tumour (DNET); cancer stem cells (CSCs); drug resistance

Submitted Jan 10, 2022. Accepted for publication May 18, 2022.
doi: 10.21037/tp-22-19
View this article at: https://dx.doi.org/10.21037/tp-22-19

Introduction

Dysembryoplastic neuroepithelial tumours (DNETs) are rare intracranial tumours that may have inconsistencies in disease progression (1,2). Several recent studies have described the molecular mutations and deregulations of a few DNET cases (3-6). Out of all 283 published DNET cases, 143 were paediatric patients (age: 0–14 years; supplementary table available at: https://cdn.amegroups.cn/static/public/tp-22-19-1.xlsx). Out of 63 DNA-examined paediatric DNET cases, 33 samples were shown

to have fibroblast growth factor receptor 1 (*FGFR1*) variants. Overall, mutations in the *FGFR1* gene have been detected in 32 different types of tumours (7). Given the complexity and heterogeneity of most central nervous system tumours (CNSTs), targeting a single gene is unlikely to be highly effective in improving survivorship (8). Thus, we investigated the status of cancer stem cell (CSC) genes associated with resilience and drug resistance in a paediatric DNET. CSCs are cancer cells that utilise stem cell pathways, enhance tumorigenesis and contribute to drug resistance, and their associated markers have been identified in several CNSTs (9-18). Data on the status of CSCs in DNETs have not been published. As such, this report presents data on several deregulated CSC genes and their variants that may be associated with a predisposition for DNET. We present the following article in accordance with the CARE reporting checklist (available at https://tp.amegroups.com/article/view/10.21037/tp-22-19/rc).

Case presentation

All procedures performed in this study were in accordance with the ethical standards of the institutional and/or national research committee(s) and with the Helsinki Declaration (as revised in 2013). Written informed consent was obtained from the patient's parents or legal guardians for publication of this case report. A copy of the written consent is available for review by the editorial office of this journal. This work was approved by the Ethical Board of King Abdulaziz University Hospital (board registration No. at the National Committee of Bio- and Medical Ethics: HA-02-J-008; project reference No. 976-12).

Patient information and clinical findings

A 6-year-old boy presented with drug-resistant focal epilepsy since the age of 2 years. He is the only child for a non-consanguineous couple and the product of an uneventful pregnancy that was delivered via caesarean section. The child's first 2 years of life were uneventful, with healthy psychomotor development without a history of febrile illness or trauma and no family history of epilepsy.

The beginning of his seizures was brief absence-like, which lasted for 15–20 s, occurring at a frequency of 4–5 times per week. Subsequently, the seizures became prolonged and of focal onset daily with an impaired conscious level with secondary generalisation occasionally once or twice a month. The patient initially had a good response with valproate for 6 months, but his seizures recurred, and several antiepileptic medications were added, with no positive response. Subsequently, levetiracetam, clobazam and carbamazepine were added, resulting in partial control. However, the patient still suffered several seizures a week. The patient's physical and neurological examinations were unremarkable.

An electroencephalogram (EEG) showed important lateralising interictal epileptiform discharges in the posterior right hemisphere. Long-term video-EEG monitoring revealed that the focal impaired-awareness seizures coincided with ictal EEG activities arising from a right posterior hemispheric lesion. A magnetic resonance imaging (MRI) scan revealed an extensive lesion in the right posterior temporoparietooccipital region (PTR), disclosing hyper T2 signal intensity and hypo T1 signal intensity without contrast enhancement or mass effect. The lesion measured 6.0 cm × 3.0 cm × 2.5 cm, demonstrating focal cortical thickening and a blurred grey-white matter junction (*Figure 1A-1F*). The preoperative diagnoses were considered low-grade tumour-like DNET or focal cortical dysplasia (FCD). The child underwent right posterior temporoparietooccipital neuronavigation-assisted craniotomy in January 2016. Complete neuronavigation-assisted microsurgical resection was performed and confirmed by postoperative MRI (*Figure 1G-1I*). A histopathological examination of paraformaldehyde-fixed sections showed pathological features consistent with DNET. The examination revealed a well-demarcated, cortically located multinodular lesion (*Figure 1J,1K*), forming the so called "specific glioneuronal element". This element is composed of oligodendrocyte-like cells (OLCs) with round nuclei and clear perinuclear cytoplasmic halos, which are aligned in columns along anuclear zones of neuronal processes containing small blood vessels that are oriented perpendicularly to the cortical surface. The columns are separated by mucin-containing microcysts and a few scattered floating neurons (*Figure 1L*). Synaptophysin immunohistochemistry staining is positive in the floating neurons and neuropil-like matrix; contrastingly, small OLCs are synaptophysin negative (*Figure 1M*). The patient remained seizure-free until December 2020.

Molecular and biological analyses

DNET fresh frozen tissue is highly positive for numerous CSC markers

Consecutive sections of the patient's fresh frozen tumour were cut and immunofluorescence stained to detect CSC

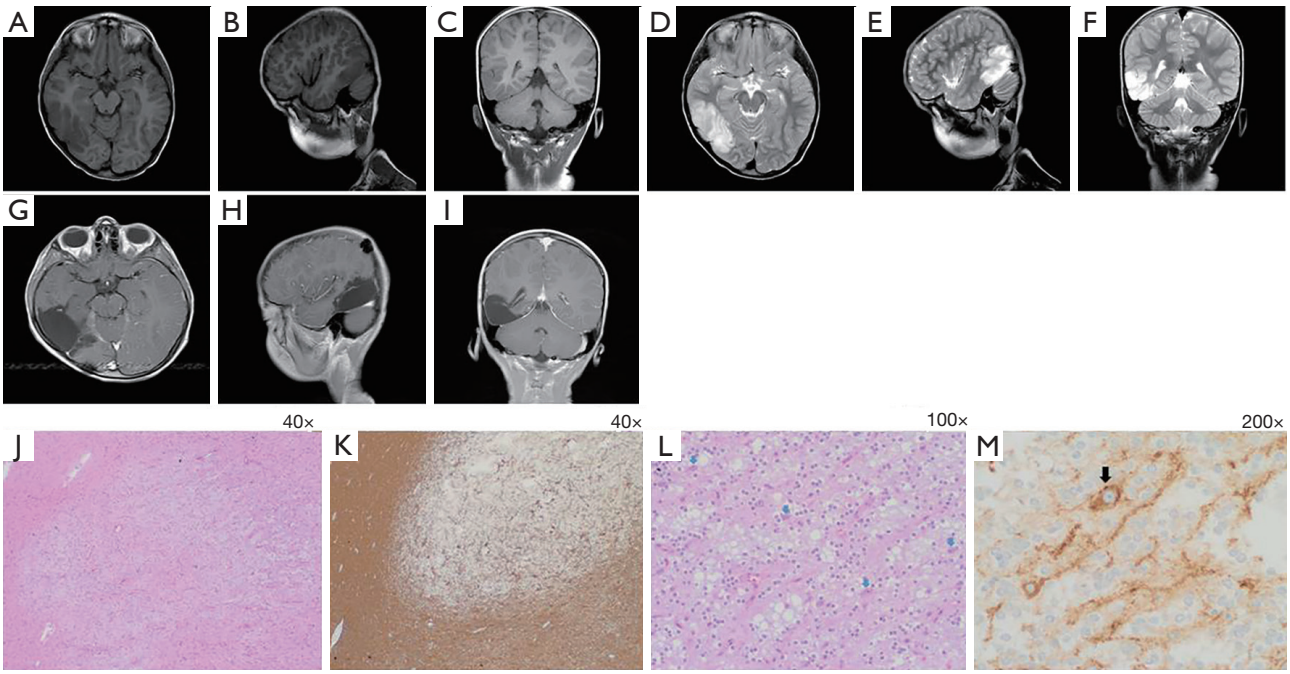

Figure 1 Patient's clinical findings. Preoperative MRI study revealed T1-weighted axial (A), parasagittal (B) and coronal (C) images demonstrating a right posterior temporoparietooccipital hypointense well-demarcated cortical thickening. The lesion showed hyperintensity on T2-weighted axial (D), parasagittal (E) and coronal (F) images. Postoperative enhanced T1-weighted axial (G), parasagittal (H) and coronal (I) MRI study revealed adequate complete resection. Tissue pathological findings illustrated in parts (J-M). (J) Low-power H&E micrograph showing a nodular lesion demonstrating a relatively well-defined borders with adjacent normal brain tissue (left side). (K) GFAP staining of paraformaldehyde fixed tissue with relatively sharp demarcation from normal tissue (left and below sides). (L) Medium-power H&E micrograph showing the so-called "specific glioneuronal element", characterised by OLCs aligned in columns along anuclear zones of neuronal processes containing small blood vessels. The columns are separated by microcysts containing mucin and few scattered floating neurons (arrows). (M) Synaptophysin staining is positive in a floating neuron (arrow) and neuronal processes, whereas small OLCs are negative. Inlet: synaptophysin immunohistochemistry: neuropil-like background. GFAP, glial fibrillary acidic protein; MRI, magnetic resonance imaging; OLCs, oligodendrocyte-like cells.

markers previously associated with CNSTs (13), as shown in *Figure 2*, Figure S1 and Supplementary Methods File 1 (Appendix 1). Staining revealed vast differences for Ki67 positivity across tumour regions. Positive cells were grouped into particular regions of the tumour, with 2.4%±0.9% in positive regions. Low expression was detected for Notch receptor 1 (NOTCH1; 13.6%±6.2%) and nuclear SRY-Box transcription factor 2 (SOX2; 6.2%±2.8%). Medium expression was detected for catenin beta 1 (CTNNB1; 34.8%±16.8%), NUDC domain containing 3 (NUDCD3; 42.0%±29.1%), oligodendrocyte transcription factor 2 (OLIG2; 37.9%±7.5%). High expression was detected for anterior gradient 2 (AGR2; 67.2%±18.3%), glial fibrillary acidic protein (GFAP; 95.3%±1.6%), vimentin (VIM; 93.7%±3.6%), tubulin beta 3 class III (TUBB3; 81.7%±9.0%) and the Wnt-signalling-related protein frizzled class receptor 9 (FZD9; 79.0%±14.4%). No expression was detected for nestin (–), prominin 1 (CD133) (–), P53 (–), or SRY-box transcription factor 11 (Sox11) (–) (images not shown).

DNET-retrieved cell line's resistance to cisplatin and expression of tumorigenic and CSC markers

In order to investigate whether the presence of CSCs in the DNET tissue might have any favourable selection for survival, a DNET cell line was retrieved from the fresh tumour mass and investigated for its drug resistance and CSC marker expression (*Figure 3*). Cells were culture adapted, had an average doubling time (DT) of 4±0.3 days, a Ki67 expression of 14.8%±5.7%, and were

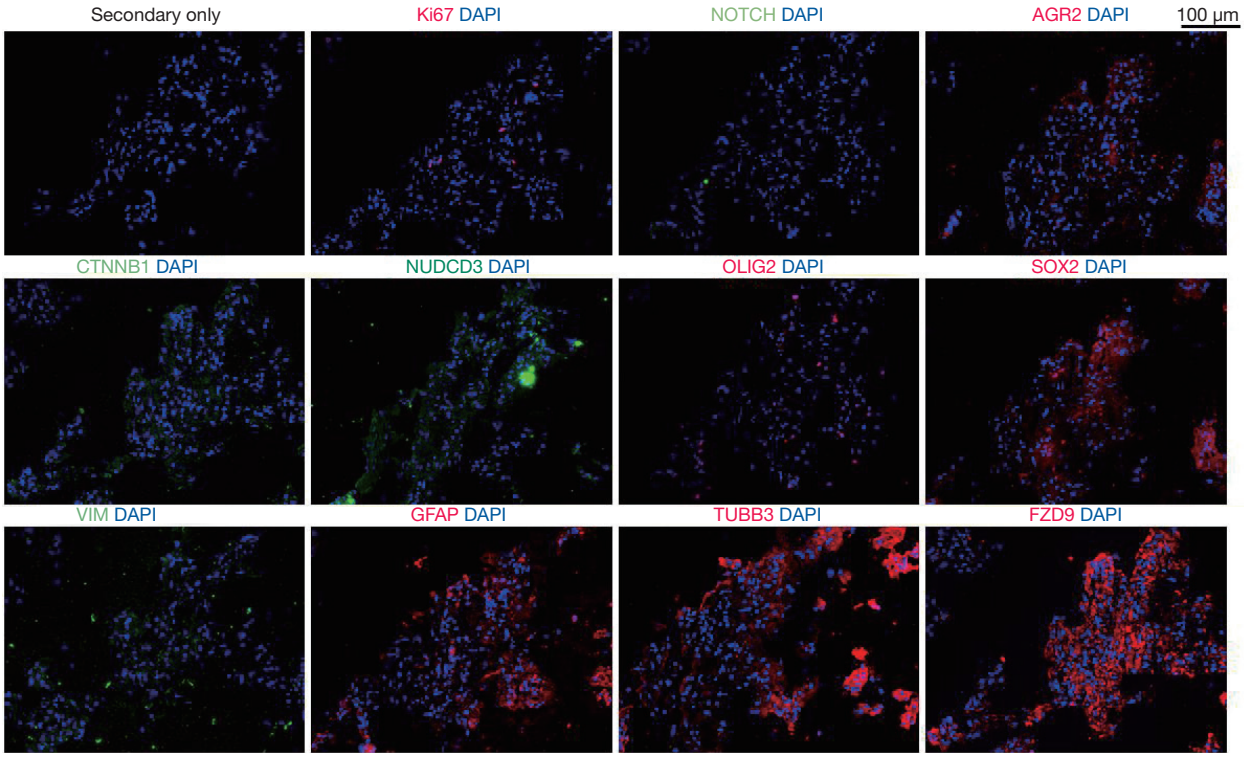

Figure 2 Immunofluorescence images for the selected markers in consecutive tissues. Shown in red are rabbit antibodies against Ki67, AGR2, OLIG2, FZD9, SOX2, GFAP and TUBB3. Shown in green are mouse antibodies against NOTCH, CTNNB1, VIM and NUDCD3. DAPI is shown in blue. All images were taken at ×20. AGR2, anterior gradient 2; CTNNB1, catenin beta 1; FZD9, frizzled class receptor 9; GFAP, glial fibrillary acidic protein; NUDCD3, NUDC domain containing 3; OLIG2, oligodendrocyte transcription factor 2; SOX2, SRY-Box transcription factor 2; TUBB3, tubulin beta 3 class III; VIM, vimentin.

grown to at least passage 15. In order to ensure the cell line was representative of the tumour, the percentage similarity of single nucleotide variants (SNVs) in exomes for DNA collected from the cell line and the corresponding tissue was compared with the percentage similarity of SNVs in exomes for DNA collected from the cell line and non-corresponding tissues (*Figure 3B*). The previously published cell line, Jed38_MN (12,19), had 98.5% similarity between SNVs in the cell line and its corresponding tissue. It had an average of 56.3% similarity with SNVs in exomes of 13 other meningioma tissues retrieved from other patients. In comparison, the Jed99_DNET cell line had an 89.2% similarity between SNVs in the cell line and its corresponding tissue, a 32.4% average similarity with SNV in the exomes of 14 meningioma tissues retrieved from other patients, and 16.4% average similarity with SNVs detected in the blood of the aforementioned patient. Statistical analysis indicated that the percentage similarity between SNVs in the exomes of DNA collected from the cell line and their corresponding tissues is significantly higher than the percentage similarity of SNVs in the exomes of DNA collected from the cell line and non-corresponding tissues ($P<0.001$).

Next, the Jed99_DNET cell line was subjected to the clonogenic assay to check for its ability to form clones in culture and resist drug treatment, both characteristics of aggressiveness. Drug treatment with cisplatin and taxol for passages 8, 10 and 12 indicated an IC_{50} of 7.1 µM for cisplatin and an IC_{50} of 3.04 nM for taxol (*Figure 3C*); notably, several clones survived at doses higher than IC_{50}. In order to address whether the retrieved cells were tumorigenic, cells were immunofluorescence stained for the tumorigenic proto-oncogene (BMI) and metastatic marker (AGR2); results were highly positive for both (*Figure 3D*). Cells also had high expression (>50%) for several CSC markers, including VIM, FZD9, CTNNB1, GFAP, NUDCD3, TUBB3 and OLIG2 (particularly localised in the nuclear envelope). Notably, the expression

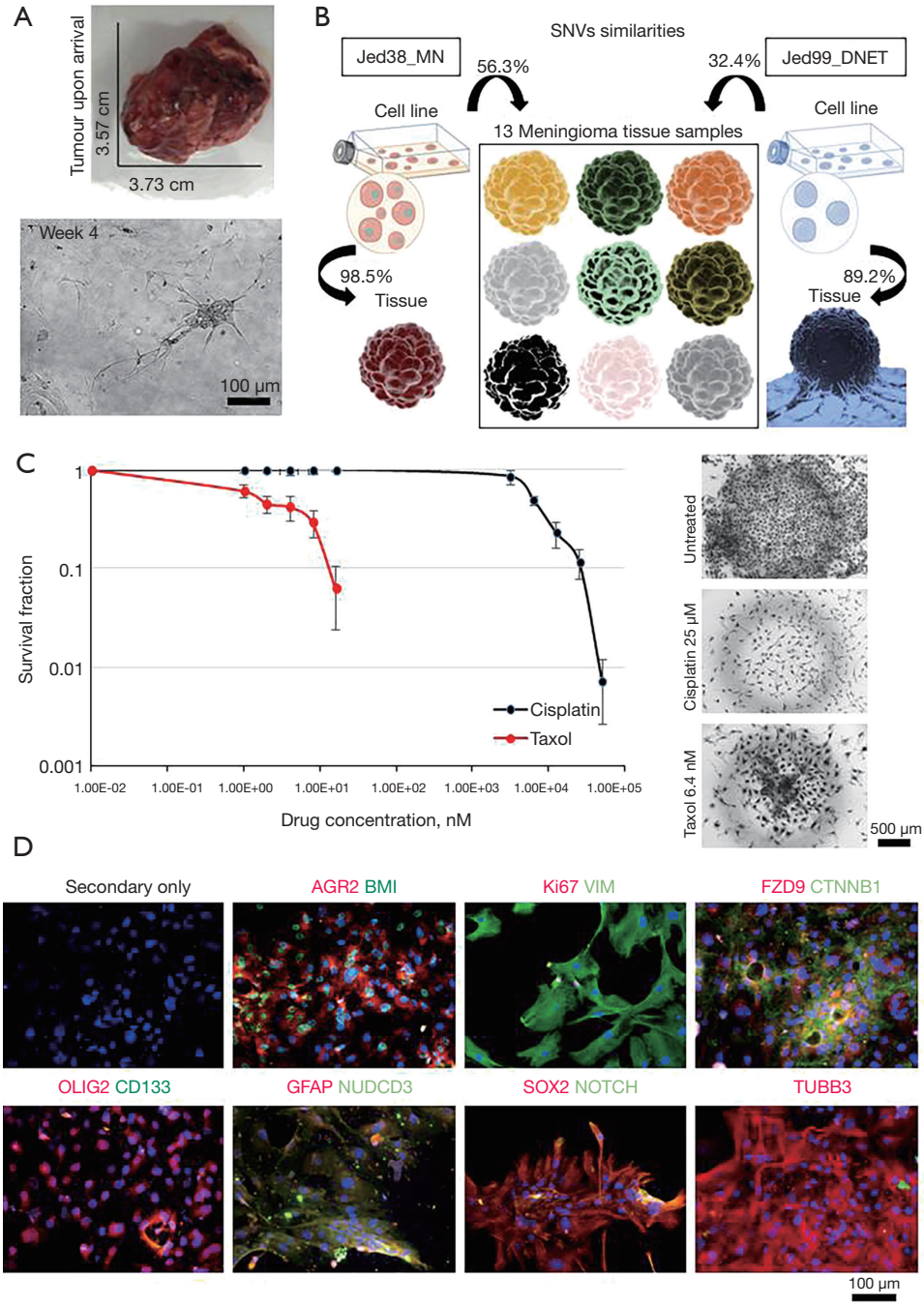

Figure 3 Characterisation of the Jed99_DNET cell line. (A) Original tumour and live cells. (B) A representative figure showing the percentage similarity of SNVs in exomes for DNA retrieved from cell lines and tissues. The previously published meningioma cell line Jed38_MN was used for a comparative purpose. (C) Drug treatment with cisplatin and taxol using the clonogenic assay for passages 8, 10 and 12 and images of drug-resistant clones taken at ×5 are shown. (D) Immunofluorescence co-staining of live cells. Shown in red are rabbit-based antibodies against AGR2, Ki67, FZD9, OLIG2, GFAP, SOX2, and TUBB3. Shown in green are mouse-based antibodies against BMI, VIM, CTNNB1, CD133, NUDCD3, and NOTCH. DAPI is shown in blue. All images were taken at ×20. AGR2, anterior gradient 2; BMI, BMI1 proto-oncogene; CTNNB1, catenin beta 1; DNET, dysembryoplastic neuroepithelial tumour; FZD9, frizzled class receptor 9; GFAP, glial fibrillary acidic protein; NUDCD3, NUDC domain containing 3; OLIG2, oligodendrocyte transcription factor 2; SNVs, single nucleotide variants; SOX2, SRY-Box transcription factor 2; TUBB3, tubulin beta 3 class III; VIM, vimentin.

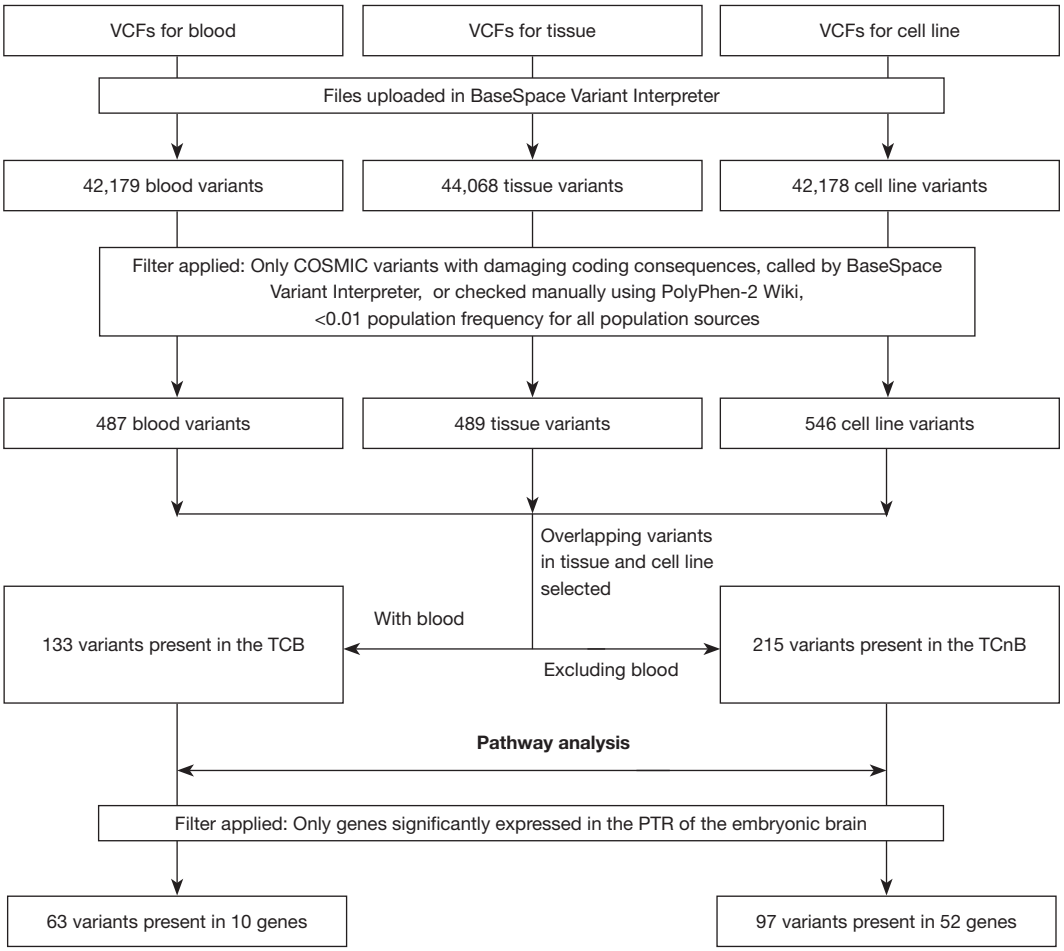

Figure 4 Analysis workflow for the bioinformatics processing of files generated for the whole exome sequencing. Two critical filters applied based on genes currently listed in the COSMIC data base (7), and genes that have been previously shown to be significantly expressed in the PTR of the embryonic brain (20). COSMIC, catalogue of somatic mutations in cancer; PTR, posterior temporoparietooccipital region; VCF, variant call format; TCB, tissue, cell line and blood; TCnB, tissue and cell line but not the blood.

of NOTCH1 and nuclear SOX2 were low (<20%), and CD133 was not expressed.

Whole exome sequencing (WES) analysis of the tissue, cell line and blood (TCB)

Having detected deregulated expressions of important CSC markers in both the tissue and corresponding cell line, we investigated the presence of in-common TCB (14) variants for genes listed in the common catalogue of somatic mutations in cancer (COSMIC) database, identified in the SCDevDB database (7,20). The pipeline used for a variant call format (VCF) analysis is shown in *Figure 4*. Supplementary tables (available at https://cdn.amegroups.cn/static/public/tp-22-19-2.xlsx) and Figure S2 show the COSMIC variants for each sample, their basic features and affected pathways. Supplementary table (available at https://cdn.amegroups.cn/static/public/tp-22-19-3.xlsx) shows selected rare COSMIC variants with damaging coding consequences present in both the tissue and the corresponding cell line Jed99_DNET, but not in the blood (TCnB). This table shows details for somatic related variants including a variant in the insulin growth factor-2 binding protein 3 (*IGF2BP3)* gene.

The final filtration selected TCB-COSMIC variants for genes previously published to be relevant for the development of the PTR (20), since the tumour was located in PTR. Ten COSMIC-PTR genes were identified (*Table 1*); these included the cell division cycle 27 (*CDC27*)

Table 1 PTR-COSMIC-damaging variants detected in TCB of Jed99_DNET

Gene Symbol	Description	Function	COSMIC
ATN1	Atrophin 1	BP: GO:0051402 neuron apoptotic process	COSM431781
CDC27	Cell division cycle 27	BP: GO: 0045842 positive regulation of mitotic metaphase/anaphase transition; HGS: (M5893) HALLMARK MITOTIC SPINDLE; (M5901) HALLMARK G2M CHECKPOINT; (M5945) HALLMARK HEME METABOLISM	COSM4130311, COSM4130259, COSM5453105, COSM4268063, COSM4130195, COSM4130201, COSM4130207, COSM4130213, COSM4130215, COSM4130217, COSM436751, COSM5611630, COSM4130221, COSM6291465, COSM4130241, COSM4130243, COSM4130245, COSM5764327, COSM3742283, COSM4130257, COSM4130301, COSM4130307, COSM4130309, COSM4130313
CTBP2	C-terminal binding protein 2	BP: GO: 0048386 positive regulation of retinoic acid receptor signaling pathway; CP: (M5493) WNT SIGNALING	COSM5620575, COSM5468715, COSM5346315, COSM145279, COSM5021689, COSM3773526, COSM5620563, COSM5620565, COSM213712, COSM328281, COSM2021368, COSM4175021, COSM5703489, COSM5764563, COSM4144437, COSM4144443, COSM1603121, COSM4610155, COSM1600226, COSM4144449, COSM4144451, COSM4144455
FRG1	FSHD region gene 1	BP: GO: 0006364 rRNA processing	COSM6029312, COSM4005732
HYDIN	HYDIN axonemal central pair apparatus protein	BP: GO: 1904158 axonemal central apparatus assembly	COSM146271, COSM5958323, COSM1379438, COSM4129291
IGSF3	Immunoglobulin superfamily member 3	BP: GO: 0032808 lacrimal gland development; HGS: (M5945) HALLMARK HEME METABOLISM	COSM4142216
KMT2C	Lysine methyltransferase 2C	BP: GO: 0097692 histone H3-K4 monomethylation	COSM216053, COSM4161993, COSM4162005, COSM4162009
NCOR1	Nuclear receptor corepressor 1	BP: GO: 0045820 negative regulation of glycolytic process; CP: (M13) PID ERBB4 PATHWAY; (M288) PID HES HEY PATHWAY; (M17) PID NOTCH PATHWAY	COSM5574208
PABPC1	Poly(A) binding protein cytoplasmic 1	BP: GO: 2000622 regulation of nuclear-transcribed mRNA catabolic process, nonsense-mediated decay; HGS: (M5949) HALLMARK PEROXISOME; (M5926) HALLMARK MYC TARGETS V1	COSM6201671, COSM485880, COSM6276973
VWF	von Willebrand factor	BP: GO:0007597 blood coagulation, intrinsic pathway; CP: (M3008) NABA ECM GLYCOPROTEINS; HGS: (M5946) HALLMARK COAGULATION; (M5915) HALLMARK APICAL JUNCTION	COSM6417961

COSMIC codes last checked 01/11/2021. All selected genes were significantly associated with the development of the posterior temporoparietooccipital (occipital lobe, parietal lobe, temporal lobe) region of the brain during embryogenesis ($P<0.01$) (20). All attributed functions were identified by Metascape. BP, biological process (GO); CP, canonical pathways; COSMIC, catalogue of somatic mutations in cancer; DNET, dysembryoplastic neuroepithelial tumour; GO, Gene Ontology; HGS, hallmark gene sets; PTR, posterior temporoparietooccipital region; TCB, tissue, cell line and blood.

and C-terminal binding protein 2 (*CTBP2*) genes.

Discussion

Our case report elucidated the combined deregulated expression of several CSC markers in a paediatric DNET. Immunofluorescence analysis of the tissue and its corresponding cell line showed positive expressions of several CSC markers. High expressions of GFAP, microtubule-associated protein 2 and synaptophysin were previously observed in reported malignant transformation cases of DNETs (21,22). It is worth mentioning that the positivity of a single marker, such as GFAP, cannot be considered indicative of the differentiation into the glial pathway since also OLIG2 and TUBB3 were positive in the corresponding consecutive sections. Thus, in this case, the triple positivity more likely reflects the progenitor-like state of cancer cells, an observation previously seen in meningioma tissues (12).

The biological characteristics of the corresponding primary cell line, Jed99_DNET, displayed relatively well-established *in vitro* cell growth. The comparative analysis of the SNVs indicated that DNA collected from the primary cell line is highly representative of the corresponding tissue's DNA. Critically, cells were highly positive for BMI and AGR2, indicating that the recovered cells were tumorigenic. Additionally, several tested stem cell markers were highly positive and mimicked patterns seen *in situ*. Consistent with the notion that CSCs are associated with drug resistance, early passage cells were also relatively drug-resistant, particularly to cisplatin.

Ten TCB-COSMIC-PTR genes had damaging variants; the most altered gene, *CDC27*, possessed 24 variants. *CDC27* has an important role as a positive regulator of the mitotic metaphase/anaphase transition and has been shown to be a critical subunit of the anaphase-promoting complex/cyclosome (APC) (23). Two well-studied functional regions of the protein were identified, namely, the anaphase-promoting complex 3 (ApC3) and tetratricopeptide repeat (TPR) regions, which are needed to stabilise interactions with the APC complex (24). The COSMIC database includes several deregulations and mutations of this gene that are associated with embryonal tumours, suggesting a critical and primal role of this gene in driving paediatric tumorigenesis (7,25,26). Furthermore, previously identified mutations in *CDC27* were shown to significantly correlate with progressive disease, low overall survival and disease-free survival (23,27). The second gene with the most frequent TCB variants was the *CTBP2* gene. The protein is a transcriptional corepressor capable of sensing the levels of cytosolic nicotinamide adenine dinucleotide (NAD) + hydrogen (H) (NADH) and is thought to reside in the nucleus. The deletion of this gene was shown to lead to embryonic lethality, and the involvement of *CTBP2* in the Wnt signalling pathway have been shown (28). Further functional large cohort studies are necessary to clarify whether either *CDC27 or CTBP2* are critical markers for aggressive DNETs.

Unfortunately, one limitation is the inability to test a large number of samples under the same experimental conditions, as these tumours are rare. In our sample, no COSMIC variations were found in the tissue's DNA for *FGFR1*, *BRAF* or *NF1* genes, which is consistent with the aforementioned information mentioned in the introduction and the supplementary table (available at https://cdn.amegroups.cn/static/public/tp-22-19-1.xlsx), as not all histopathologically identified paediatric DNETs have mutations in these genes. However, several variants were detected in other genes that most likely have redundant functions in pathways associated with the aforementioned genes, which may have a parallel effect to *FGFR1* mutations. For example, a TCnB COSMIC variant was detected in the *IGF2BP3* gene. Both FGFR1 and IGF2BP3 influence the phosphatidylinositol 3-kinase/mitogen-activated protein kinase (PI3K/MAPK) pathway (29,30), therefore perhaps mutations in these genes may have redundant effects on this pathway, which may prove to be important in DNETs.

To our knowledge, the work described in this report assesses for the first time the presence of CSCs in a paediatric DNET. High expressions of several CSC genes were observed in both *in situ* and the corresponding cell line. Primary cells were relatively drug-resistant, particularly to cisplatin. Using WES analysis, while focusing on the TCB variants of essential developmental genes of the brain's PTR, identified several genes (e.g., the mitotic regulator gene *CDC27* and the Wnt signalling-related gene *CTBP2*). Further functional large cohort studies are necessary to clarify the diagnostic and prognostic applications of these observations.

Acknowledgments

We would like to thank the KFMRC administration and technical departments for their support, the former director Dr. Ghazi Damanhouri and Dr. Mohammed Jan from the Paediatric Department at KAU Hospital.

Funding: This work was funded by the Dean of Scientific Research, King Abdulaziz University, KSA (G: 489-141-1440).

Footnote

Reporting Checklist: The authors have completed the CARE reporting checklist. Available at https://tp.amegroups.com/article/view/10.21037/tp-22-19/rc

Peer Review File: Available at https://tp.amegroups.com/article/view/10.21037/tp-22-19/prf

Conflicts of Interest: All authors have completed the ICMJE uniform disclosure form (available at https://tp.amegroups.com/article/view/10.21037/tp-22-19/coif). The authors have no conflicts of interest to declare.

Ethical Statement: The authors are accountable for all aspects of the work in ensuring that questions related to the accuracy or integrity of any part of the work are appropriately investigated and resolved. All procedures performed in this study were in accordance with the ethical standards of the institutional and/or national research committee(s) and with the Helsinki Declaration (as revised in 2013). Written informed consent was obtained from the patient's parents or legal guardians for publication of this case report. A copy of the written consent is available for review by the editorial office of this journal. This work was approved by the Ethical Board of King Abdulaziz University Hospital (board registration no. at the National Committee of Bio- and Medical Ethics: HA-02-J-008; Project reference No. 976-12).

References

1. Chiang JCH, Harreld JH, Tanaka R, et al. Septal dysembryoplastic neuroepithelial tumor: a comprehensive clinical, imaging, histopathologic, and molecular analysis. Neuro Oncol 2019;21:800-8.
2. Luzzi S, Elia A, Del Maestro M, et al. Dysembryoplastic Neuroepithelial Tumors: What You Need to Know. World Neurosurg 2019;127:255-65.
3. Lucas CG, Gupta R, Doo P, et al. Comprehensive analysis of diverse low-grade neuroepithelial tumors with FGFR1 alterations reveals a distinct molecular signature of rosette-forming glioneuronal tumor. Acta Neuropathol Commun 2020;8:151.
4. Rivera B, Gayden T, Carrot-Zhang J, et al. Germline and somatic FGFR1 abnormalities in dysembryoplastic neuroepithelial tumors. Acta Neuropathol 2016;131:847-63.
5. Surrey LF, Jain P, Zhang B, et al. Genomic Analysis of Dysembryoplastic Neuroepithelial Tumor Spectrum Reveals a Diversity of Molecular Alterations Dysregulating the MAPK and PI3K/mTOR Pathways. J Neuropathol Exp Neurol 2019;78:1100-11.
6. Zakrzewska M, Gruszka R, Stawiski K, et al. Expression-based decision tree model reveals distinct microRNA expression pattern in pediatric neuronal and mixed neuronal-glial tumors. BMC Cancer 2019;19:544.
7. Tate JG, Bamford S, Jubb HC, et al. COSMIC: the Catalogue Of Somatic Mutations In Cancer. Nucleic Acids Res 2019;47:D941-7.
8. Melcher V, Kerl K. The Growing Relevance of Immunoregulation in Pediatric Brain Tumors. Cancers (Basel) 2021;13:5601.
9. Patel AP, Tirosh I, Trombetta JJ, et al. Single-cell RNA-seq highlights intratumoral heterogeneity in primary glioblastoma. Science 2014;344:1396-401.
10. Venteicher AS, Tirosh I, Hebert C, et al. Decoupling genetics, lineages, and microenvironment in IDH-mutant gliomas by single-cell RNA-seq. Science 2017;355:eaai8478.
11. Zhang L, He X, Liu X, et al. Single-Cell Transcriptomics in Medulloblastoma Reveals Tumor-Initiating Progenitors and Oncogenic Cascades during Tumorigenesis and Relapse. Cancer Cell 2019;36:302-318.e7.
12. Alamir H, Alomari M, Salwati AAA, et al. In situ characterization of stem cells-like biomarkers in meningiomas. Cancer Cell Int 2018;18:77.
13. Khan IN, Ullah N, Hussein D, et al. Current and emerging biomarkers in tumors of the central nervous system: Possible diagnostic, prognostic and therapeutic applications. Semin Cancer Biol 2018;52:85-102.
14. Hussein D, Dallol A, Quintas R, et al. Overlapping

variants in the blood, tissues and cell lines for patients with intracranial meningiomas are predominant in stem cell-related genes. Heliyon 2020;6:e05632.
15. Filbin MG, Tirosh I, Hovestadt V, et al. Developmental and oncogenic programs in H3K27M gliomas dissected by single-cell RNA-seq. Science 2018;360:331-5.
16. Magill ST, Vasudevan HN, Seo K, et al. Multiplatform genomic profiling and magnetic resonance imaging identify mechanisms underlying intratumor heterogeneity in meningioma. Nat Commun 2020;11:4803.
17. Neftel C, Laffy J, Filbin MG, et al. An Integrative Model of Cellular States, Plasticity, and Genetics for Glioblastoma. Cell 2019;178:835-849.e21.
18. Wang L, Babikir H, Müller S, et al. The Phenotypes of Proliferating Glioblastoma Cells Reside on a Single Axis of Variation. Cancer Discov 2019;9:1708-19.
19. Khan I, Baeesa S, Bangash M, et al. Pleomorphism and drug resistant cancer stem cells are characteristic of aggressive primary meningioma cell lines. Cancer Cell Int 2017;17:72.
20. Wang Z, Feng X, Li SC. SCDevDB: A Database for Insights Into Single-Cell Gene Expression Profiles During Human Developmental Processes. Front Genet 2019;10:903.
21. Heiland DH, Staszewski O, Hirsch M, et al. Malignant Transformation of a Dysembryoplastic Neuroepithelial Tumor (DNET) Characterized by Genome-Wide Methylation Analysis. J Neuropathol Exp Neurol 2016;75:358-65.
22. Matsumura N, Natsume A, Maeda S, et al. Malignant transformation of a dysembryoplastic neuroepithelial tumor verified by a shared copy number gain of the tyrosine kinase domain of FGFR1. Brain Tumor Pathol 2020;37:69-75.
23. Kazemi-Sefat GE, Keramatipour M, Talebi S, et al. The importance of CDC27 in cancer: molecular pathology and clinical aspects. Cancer Cell Int 2021;21:160.
24. Ben-David U, Amon A. Context is everything: aneuploidy in cancer. Nat Rev Genet 2020;21:44-62.
25. Håvik AL, Bruland O, Myrseth E, et al. Genetic landscape of sporadic vestibular schwannoma. J Neurosurg 2018;128:911-22.
26. Kohsaka S, Shukla N, Ameur N, et al. A recurrent neomorphic mutation in MYOD1 defines a clinically aggressive subset of embryonal rhabdomyosarcoma associated with PI3K-AKT pathway mutations. Nat Genet 2014;46:595-600.
27. Wu R, Li Q, Wu F, et al. Comprehensive Analysis of CDC27 Related to Peritoneal Metastasis by Whole Exome Sequencing in Gastric Cancer. Onco Targets Ther 2020;13:3335-46.
28. Wang DP, Gu LL, Xue Q, et al. CtBP2 promotes proliferation and reduces drug sensitivity in non-small cell lung cancer via the Wnt/β-catenin pathway. Neoplasma 2018;65:888-97.
29. Kong S, Cao Y, Li X, et al. MiR-3116 sensitizes glioma cells to temozolomide by targeting FGFR1 and regulating the FGFR1/PI3K/AKT pathway. J Cell Mol Med 2020;24:4677-86.
30. Mancarella C, Scotlandi K. IGF2BP3 From Physiology to Cancer: Novel Discoveries, Unsolved Issues, and Future Perspectives. Front Cell Dev Biol 2019;7:363.

Cite this article as: Hussein D, Alhowity A, Algehani R, Salwati AAA, Dallol A, Schulten HJ, Baeesa S, Bangash M, Alghamdi F, Saka M, Chaudhary A, Abuzenadah A. A paediatric dysembryoplastic neuroepithelial tumour (DNET) with deregulated stem cell markers: a case report. Transl Pediatr 2022;11(6):1040-1049. doi: 10.21037/tp-22-19

Supplementary

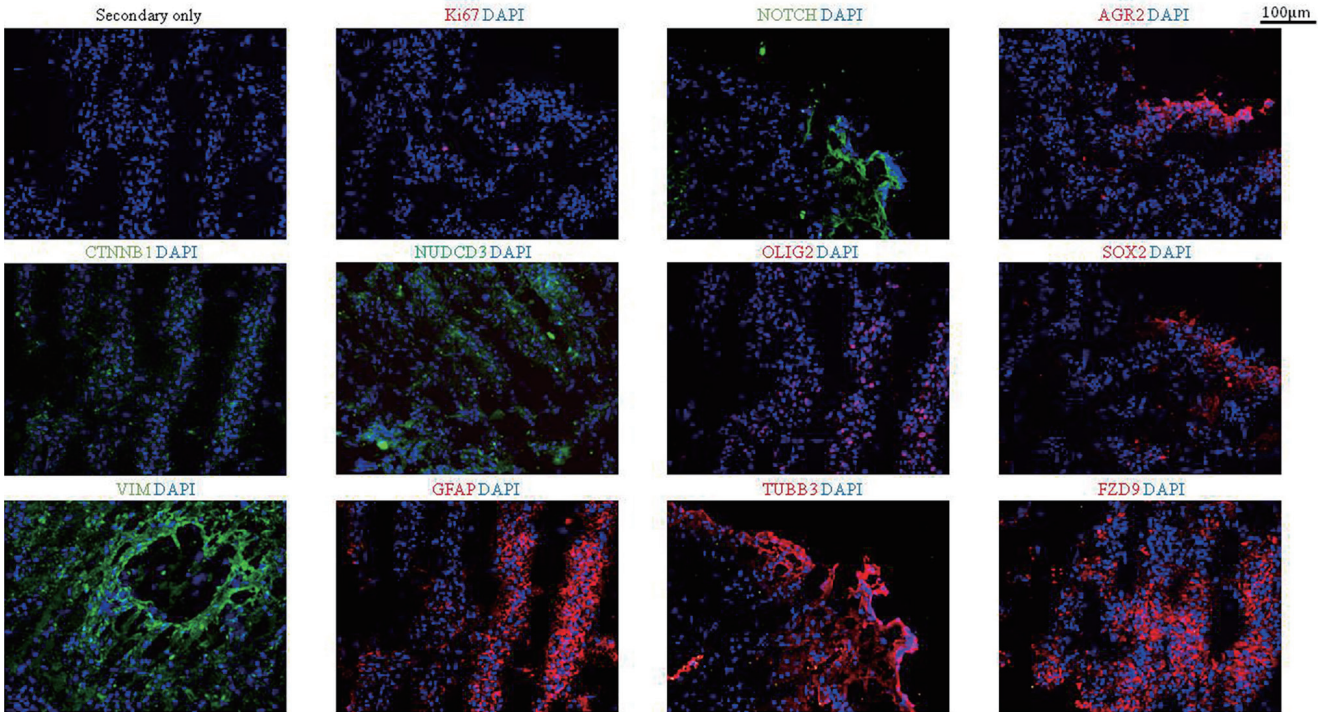

Figure S1 Immunofluorescence images showing the highest expression seen for each tested marker in the tissue. Shown in red are rabbit antibodies against Ki67, AGR2, OLIG2, FZD9, SOX2, GFAP and TUBB3. Shown in green are mouse antibodies against NOTCH, CTNNB1, VIM and NUDCD3. DAPI is shown in blue. All images were taken at ×20. AGR2, anterior gradient 2; CTNNB1, catenin beta 1; FZD9, frizzled class receptor 9; GFAP, glial fibrillary acidic protein; NUDCD3, NUDC domain containing 3; OLIG2, oligodendrocyte transcription factor 2; SOX2, SRY-Box transcription factor 2; TUBB3, tubulin beta 3 class III; VIM, vimentin.

https://dx.doi.org/10.21037/tp-22-19

Appendix 1 Material and methods

Tumour sampling and cell culture methods

Specimen collection and cell line induction were performed as previously reported (12,19). Cell line drug treatments was performed as previously described (19). The drugs' ranges for the clonogenic assay were 3.1, 6.3, 12.5, 25 and 50 µM for cisplatin, and 1, 2, 4, 8 and 16 nM for taxol.

WES analysis

Libraries were generated in the Roya Laboratories, as per their standard protocols (ThermoFisher Scientific, Massachusetts, USA). The samples had an average total read depth of 119.9× for blood, 136.3× for tissue and 113.7× for the cell line. The pipeline used for the variant call format (VCF) analysis is shown in *Figure 4*. The files were annotated in the BaseSpace Variant Interpreter (accessed on 03/02/2021). Only catalogue of somatic mutations in cancer (COSMIC) variants that had damaging coding consequences, as called by BaseSpace Variant Interpreter platform provided by Illumina, or checked manually using PolyPhen-2 Wiki, and had a population frequency of less than 0.01 for all population sources, were selected. COSMIC variants detected in tissue, cell line and blood (TCB) were selected, a process previously shown to potentially enrich for predictive, tumorigenic and progressive genes (14). A final filter was applied based on genes previously published to be relevant in the posterior temporoparietooccipital region (PTR) of embryonic brain development as outlined in the SCDevDB (20).

Pathway analysis

Biological functions and implicated pathways were interpreted by employing both Panther and Metascape platforms.

Immunofluorescence staining

Frozen tissue was sectioned to generate 10 consecutive sections at 4-µm thickness. Each section was processed as previously mentioned (12). Sections were stained with only secondary rabbit anti-Ki67 (1:200, ab16667, Abcam), rabbit anti-anterior gradient 2 (AGR2) (1:100, ab227584, Abcam), rabbit anti-oligodendrocyte transcription factor 2 (OLIG2) (1:500, ab42453, Abcam), rabbit anti-frizzled class receptor 9 (FZD9) (1:100, ab150515, Abcam), rabbit anti-SRY-box transcription factor 2 (SOX2) (1:200, 130-095-636, Miltenyi), mouse anti-NOTCH (1:100, ab44986, Abcam), mouse anti-catenin beta 1 (CTNNB1) (1:500, ab18207, Abcam), rabbit anti-glial fibrillary acidic protein (GFAP) (1:500, ab7260, Abcam), rabbit anti-tubulin beta 3 class III (TUBB3) (1:500, ab18207, Abcam), mouse anti-vimentin (1:100, ab8978, Abcam), mouse anti-NUDC domain containing 3 (NUDCD3) (1:100, ab89080, Abcam), mouse anti-nestin (1:50, ab6142, Abcam), mouse anti-CD133 (1:100, 130-092-395, Miltenyi), mouse anti-P53 (1:500, ab26, Abcam) and mouse anti-SRY-box transcription factor 11 (SOX11) (1:200, ab154138, Abcam). For each section, five coordinate-fixed dispersed regions were selected for imaging. For cell line staining, cells were co-stained with the aforementioned antibodies in the following pattern: rabbit anti-Ki67 with mouse anti-Vimentin, rabbit anti-FZD9 with mouse anti-CTNNB1, rabbit anti-SOX2 with mouse anti-NOTCH, rabbit anti-GFAP with mouse anti-NUDCD3, rabbit anti-OLIG2 with mouse anti-CD133, rabbit anti-TUBB3 and rabbit anti-AGR2 with mouse anti-BMI1 proto-oncogene (BMI) (1:100, ab14389, Abcam). All images were taken and processed as previously described (12). Manual counting was performed twice by two independent scientists for three randomly selected regions, and indications for positivity for each marker and final counts were confirmed with a neuropathologist.

Statistical analysis of the data

The results were analysed using SPSS version 21.0. The percentage similarity of single nucleotide variants (SNVs) in exomes for DNA collected from cell line and tissue was calculated as: the number of unfiltered SNVs in exomes present in both DNA collected from the cell line and the tissue, as a percentage fraction of the total number of unfiltered SNVs present in the tissue. One sample *t*-test was used to test for significant differences between the percentage similarity of SNVs in exomes for cell line's and corresponding tissue's DNA, and the average percentage similarity of SNVs in exomes for cell line's and non-corresponding tissue's DNA.

https://dx.doi.org/10.21037/tp-22-19

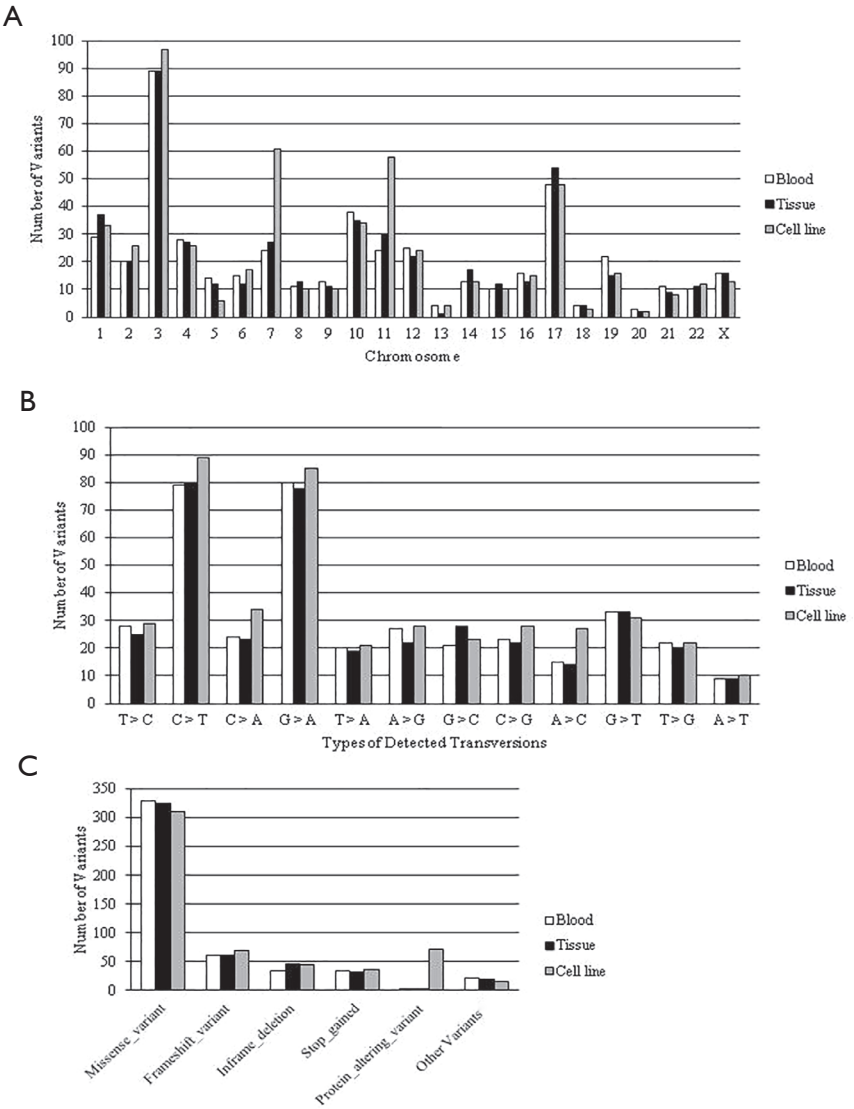

Figure S2 Basic characteristics of the COSMIC variants detected in each of the blood, tissue and cell line. (A) Number of variants detected in each chromosome. (B) Types of detected mutations in the exomic regions. (C) Number of all detected variant types based on their consequence. All selected variants had PolyPhen-damaging consequences, according to BaseSpace or PolyPhen-2 Wiki. COSMIC, catalogue of somatic mutations in cancer.

https://dx.doi.org/10.21037/tp-22-19